





## Article

# Waste By-Product of Grape Seed Oil Production: Chemical Characterization for Use as a Food and Feed Supplement

Veronica D'Eusanio <sup>1,\*</sup> , Daniele Malferrari <sup>1,2</sup> , Andrea Marchetti <sup>1,2,3</sup> , Fabrizio Roncaglia <sup>1,3</sup>   
and Lorenzo Tassi <sup>1,2,3,\*</sup> 

<sup>1</sup> Department of Chemical and Geological Sciences, University of Modena and Reggio Emilia, 41125 Modena, Italy

<sup>2</sup> Interdepartmental Research Center BIOGEST-SITEIA, University of Modena and Reggio Emilia, 42124 Reggio Emilia, Italy

<sup>3</sup> National Interuniversity Consortium of Materials Science and Technology (INSTM), 50121 Firenze, Italy

\* Correspondence: veronica.deusanio@unimore.it (V.D.); lorenzo.tassi@unimore.it (L.T.)

**Abstract:** Among the waste materials of wine production, grape seeds constitute an important fraction of the pomace, from which the precious edible oil is extracted. The residual mass from oil extraction, the defatted grape seeds (DGS), can be destined for composting or valorized according to the circular economy rules to produce pyrolytic biochar by gasification or pellets for integral energy recovery. Only a small quantity is used for subsequent extraction of polyphenols and tannins. In this study, we performed a chemical characterization of the DGS, by applying spectroscopic techniques (ICP-OES) to determine the metal content, separation techniques (HS-SPME-GC-MS) to evaluate the volatile fraction, and thermal methods of analysis (TGA-MS-EGA) to identify different matrix constituents. Our main goal is to obtain information about the composition of DGS and identify some bioactive compounds constituting the matrix in view of possible future applications. The results suggest that DGS can be further exploited as a dietary supplement, or as an enriching ingredient in foods, for example, in baked goods. Defatted grape seed flour can be used for both human and animal consumption, as it is a source of functional macro- and micronutrients that help in maintaining optimal health and well-being conditions.

**Keywords:** food waste; defatted grape seeds; dietary fibers; recycle; nutrient recovery; biorefinery; proximate composition; ICP-OES; HS-SPME-GC-MS; TGA-MS-EGA



**Citation:** D'Eusanio, V.; Malferrari, D.; Marchetti, A.; Roncaglia, F.; Tassi, L. Waste By-Product of Grape Seed Oil Production: Chemical Characterization for Use as a Food and Feed Supplement. *Life* **2023**, *13*, 326. <https://doi.org/10.3390/life13020326>

Academic Editors: Milka Mileva and Lúcia R. Rodrigues

Received: 13 December 2022

Revised: 19 January 2023

Accepted: 23 January 2023

Published: 24 January 2023



**Copyright:** © 2023 by the authors. Licensee MDPI, Basel, Switzerland. This article is an open access article distributed under the terms and conditions of the Creative Commons Attribution (CC BY) license (<https://creativecommons.org/licenses/by/4.0/>).

## 1. Introduction

It is well known that the agri-food sector produces a large amount of cellulosic by-products [1]. To address the climate emergency and reduce the environmental impact, agro-industrial waste from mechanical, chemical, or biological processes can be used for new products and applications [2]. These recovery and enhancement activities are the basis of the circular economy, aiming at “zero waste” society, in perfect agreement with Agenda 2030 [3,4]. In this regard, fruit processing by-products generally account for more than 50% of the fresh product, and these wastes often have a higher content of nutritive and functional molecules than the starting vegetables [5]. Compared to this trend, wine production is no exception, as the waste material, the whole pomace, constitutes about 50% on a fresh basis [6].

Grape is a non-climacteric fruit cultivated in temperate zones practically all over the world. According to the Food and Agriculture Organization (FAO), global grape production in 2020 was 78 million tons, of which approximately 71% was used for winemaking ([www.FAO.org](http://www.FAO.org)). The larger production occurs in Europe, with more than 23 million tons annually. Grape juice extraction leads to the formation of large quantities of important by-products and organic residues [7], including pomace, seeds, stems, yeast, and pruning, which are not sufficiently valued as highly profitable waste. Only a few quantities of

these biomasses are used as compost for fertilization [8,9], as animal feed [7,10,11], or for the generation of other products [12,13]. Among these, the seeds have greater application importance, since grapeseed oil, which is appreciated in both the cosmetic and food sectors, is extracted from them [14,15]. In terms of composition, grape seeds represent a particularly complex waste material: they contain some valuable substances, mainly phenolic compounds (i.e., flavonoids), and vegetable oil, along with natural fibers, proteins, carbohydrates, and other micro-components [14,16,17]. Flavonoids, which are isolated unsaponifiable chemicals, play an important role in the inhibition of carcinogenesis, mutagenesis, and cardiovascular diseases and exhibit activities against peptic ulcers and several dermal disorders, such as acne and dermatitis [14,18–21]. The chemo-preventive and anti-cancer efficacy of grape seeds has led to the diffusion of health and dietary supplements in the form of capsules or tablets [21]. Phenolic compounds are not particularly soluble in lipids at the process temperature required to obtain grapeseed oil. Therefore, despite the high phenolic content of grape seeds, it has been established that only a minor part of these important antioxidants is transferred to the pressed oil [7,22,23]. In addition, the yield of this process is particularly low (in the range of 100 g oil/kg seeds). Therefore, a large quantity of treated seeds remains wasted [6,24]. In this framework, this waste sub-fraction, the defatted grape seeds (DGS), has been examined, with the belief that it could become an End-of-Waste, because of its numerous residual phytochemicals.

Several studies have examined the phenolic content of DGS [7,25], but the evaluation of the volatile fraction is little reported. The volatile compounds released by a material can provide valuable information about the chemical composition of the material itself, as they are mainly formed by different degradative processes starting from the native constituent compounds [26,27]. Moreover, the analysis of the volatile fraction is closely related to the aromatic profile, which is particularly important in the food context, as well as in the cosmeceutical and fragrance industries [26]. Headspace solid-phase micro-extraction (HS-SPME) was selected because it is a relatively cheap, solventless, fast, and reproducible technique [28], which is widely used for the analysis of the volatile profile of many fruits, vegetables, and beverages [29]. In addition, SPME methodology requires small sample amounts, and its coupling with gas chromatography and mass spectrometry (GC-MS) provides high sensitivity.

Some studies concerning the thermogravimetric analyses coupled with evolved gases analysis (TGA-MS-EGA) of grape seeds are reported in the literature [30–32]. However, there is no evidence regarding the thermal degradation and pyrolytic behaviour of our lignocellulosic matrix, (i.e., the DGS sample). Since it contains a large amount of precious organic constituents and a high-energy content, its conversion into renewable energy could be an important field to explore. The use as an energy source of precious biomass far from the degradation and fermentation processes typical of organic waste is a rather controversial issue, as solutions could be explored to profitably insert it into the human food supply chain. On the other hand, DGS has huge potential in this regard, as it is a waste material with no further use in the food industry. Therefore, a detailed exploration of its thermal behaviour, including the characterization of gases released by combustion could provide valuable information about the composition of the matrix [33], in particular by estimating the hemicellulose, cellulose, and lignin content.

The defatted grape seed samples were supplied by a grape seed oil company, Randi Group (Faenza, Italy). This company fully exploits the marc (French word for pomace), which is the starting point for obtaining various by-products. The marc is washed in hot water to obtain an alcoholic liquid. The latter is sent to the distillation plant, where it is concentrated to approximately 96% ethanol. This product is marketed as a raw alcohol for industrial use, or it can undergo a second distillation and “purification” phase and be transformed into food-grade ethyl alcohol. The alcoholic liquid is separated from its tartaric component, which is sent to the calcium tartrate production plant and later to the tartaric acid production plant. The exhausted marc, stripped of its alcoholic and tartaric constituents, is screened and sieved to extract seeds. The latter are then dried and pressed

to extract the crude oil. The waste material from this process, the DGS of our interest, is used as fuel in cogeneration plants and to produce grape seed pellets. The crude oil is then sent to the refining plant, where, by means of exclusively physical and mechanical processes, it is transformed into grape seed oil. It is important to note that grape seeds are not subjected to preliminary washing. It follows that this waste material can reasonably contain residual traces of molecules highly present in the marc, such as sugars, amino acids, and organic acids. Moreover, among the various manipulations undergone by the matrix, drying heat treatment certainly leads to the modification of its composition and the volatile fraction.

On the other hand, other extraction techniques do not lead to a significant alteration in the composition of the waste product, the DGS. Among the grape seed oil extraction methods, hot pressing leads to greater deterioration of the matrix, because of the high temperatures adopted in the roasting phase [34,35]. The result is also an extremely poor-quality oil, especially for the low content of antioxidants. The main advantages of this technique are the extremely high extraction yield and low equipment cost [35]. On the other hand, supercritical fluid extraction (SFE) allows excellent extraction yields and high oil quality, as it favours the co-extraction of polyphenols [35–37]. It follows that the defatted grape seeds are also preserved in all precious thermolabile or unstable molecules that are inevitably lost during hot pressing. The main disadvantage of SFE is its extremely high cost, which has prevented its extensive application in large-scale production. Therefore, it is important to enhance a waste product that, although impoverished by heat treatment, is certainly more abundant thanks to the greater diffusion of the hot-pressing method.

Defatted grape seed flour has already been exploited in the market as a dietary supplement, or as a healthy food-enriching ingredient. The most common use is the enrichment of cereal flours, bakery products, and snacks to reduce the content of starches and sugars in the finished products and enrich them with antioxidants, polyphenols, and minerals. In this way, baked goods containing DGS flour acquire the label of “low-calorie food” due to the significant presence of non-digestible fiber [38]. Therefore, the main goal of this study was to obtain detailed information about the chemical composition of the DGS to evaluate its possible use in industrial sectors other than food and feed, such as cosmeceuticals and pharmaceuticals. In fact, we believe that this matrix is still little studied while, on the other hand, it has enormous potential and thus deserves greater interest.

## 2. Materials and Methods

### 2.1. Sample Preparation

Defatted grape seeds were obtained from a local company (Randi Group, <https://www.randi-group.com/it/randi-group/>, accessed on 15 November 2022) which produces grape seed oil in Faenza (Italy). The low moisture content (<10 wt.%, as declared by the manufacturer and proved by TGA-MS-EGA—see below, Section 3.3) makes the matrix stable over time, and prevents the growth of mold and undesirable microorganisms. Therefore, no pre-treatment or drying procedure was required. DGS are obtained from a blend of grape seeds arriving on the company’s production platform from the wineries, regardless of the cultivar and geographical origin. Randi Group’s supply area is northern Italy (Figure S1). The company confirmed that DGS represents ~90% of the waste from grape seed oil production, in agreement with previous studies [6,7,38].

### 2.2. Proximate Composition

Moisture, ash, crude protein, and residual oil were determined following the methods recommended by the Association of Official Analytical Chemists (Anon 1990). Moisture content was determined by drying the sample at 105 °C to a constant weight. The ash content was determined using a laboratory furnace at 550 °C and the temperature was gradually increased. The Dumas method was used to determine nitrogen content, which was converted to protein content multiplying by 6.25 factor [39]. The Soxhlet method was used to determine the residual fat fraction, using petroleum ether (boiling point range

40–60 °C) as the extractant solvent. Each measurement was performed in triplicate and the results were averaged.

### 2.3. Volatile Organic Compounds Sampling: HS-SPME

Approximately 2 g of DGS sample was placed in a 7-mL vial. Extraction was performed in the sample headspace, maintained at 40 °C and for 15 min, using a DVB/CAR/PDMS fiber, 50/30- $\mu$ m film thickness (Supelco, Bellefonte, PA, USA) housed in its manual holder (Supelco Inc., Bellefonte, PA, USA). The SPME fiber was then introduced into the GC–MS splitless injector (250 °C) and the thermal desorption time was 15 min. The experimental procedure was performed on three replicate samples interspersed with a SPME blank analysis. No artifacts were observed in the SPME blank analysis.

### 2.4. GC-MS Analysis

An Agilent 6890N Network gas chromatography system coupled with a 5973N mass spectrometer (Agilent Technologies, Santa Clara, CA, USA) was used for GC-MS analysis. Chromatographic separation was performed using a DB-5MS UI column (60 m  $\times$  0.25 mm i.d., 1.00  $\mu$ m film thickness; J&W Scientific, Folsom, CA, USA). Helium (He) as the carrier gas was maintained at a constant flow rate of 1 mL/min, and the column head pressure was 15 psi. The initial oven temperature was maintained for 5 min at 40 °C, followed by a heating ramp at 8 °C/min up to 160 °C, and then at 10 °C/min to reach a final temperature of 270 °C, held for 5 min. The transfer line was maintained at 270 °C.

The electron impact (EI) at 70 eV was the ionization mode of the mass spectrometer, and the full scan acquisition mode was selected, with a  $m/z$  scan range from 25 to 300. Enhanced ChemStation software (Agilent Technologies, CA, USA) was used to analyze chromatograms and mass spectra. Tentative identification of the VOCs was achieved by comparing the mass spectra with the data system library (NIST14/NIST05/WILEY275/NBS75K) and by using web databases, such as the National Institute for Standards and Technology (NIST database <https://webbook.nist.gov>, accessed on 25 November 2022) and Mass Bank of North America (<https://mona.fiehnlab.ucdavis.edu>, accessed on 26 November 2022).

The Linear Retention Index (LRI) was used to compare our data with those reported in the literature and in the NIST Standard Reference Database. The LRI values were calculated from a solution of n-alkanes (C6, C9, C12, C14, and C16) analyzed following the same procedure as that used for the samples. Pure standards (when available) were analyzed under the same operating conditions of the sample to identify some analytes. The injection of pure standards was exploited for the identification of some analytes and analyzed the same operating condition of the samples. The amount of each identified VOC is expressed as the Total Ion Current (TIC) peak area. The results are expressed as the mean of three replicates  $\pm$  standard deviation (SD).

### 2.5. Statistical Analysis

The mean and standard deviation values were calculated using the statistical functions of Microsoft Excel software (Excel<sup>®</sup> for Microsoft Office 365, Microsoft<sup>®</sup>).

### 2.6. TG-MS-EGA Analysis

A Seiko SSC 5200 thermal analyzer (Seiko Instruments Inc., Chiba, Japan) was used to perform the thermogravimetric analysis (TGA), in an inert atmosphere. A coupled quadrupole mass spectrometer (ESS, GeneSys Quadstar 422) was used to analyze the gases released during the thermal reactions (MS-EGA) (ESS Ltd., Cheshire, UK). Sampling was performed using an inert and fused silicon capillary system, which was heated to prevent condensation. The intensity of the signal of selected target gases was collected in multiple ion detection mode (MID); a secondary electron multiplier operating at 900 V collected in multiple ion detection mode (MID) the intensity of the signal of selected target gases. The signal intensities of  $m/z$  ratios of 18 for H<sub>2</sub>O, 44 for CO<sub>2</sub>, 30 for NO, and 64 for SO<sub>2</sub> were measured, respectively, where  $m/z$  is the ratio between the mass number and the charge of



the ion. The heating conditions were 20 °C/min in the thermal range of 25–1000 °C using ultrapure He at a flow rate of 100 µL/min as the purging gas.

### 2.7. Mineral Analysis and ICP-OES Determinations

The sample (DGS) was subjected to microwave acid digestion for dissolution. The element content was quantified by inductively coupled plasma-optical emission spectroscopy (ICP-OES), following the standardized procedures previously reported in other studies [40–42]. A Perkin–Elmer ICP-OES (model Optima 4200 DV) instrument equipped with an ultrasonic nebulizer (Cetac Technologies Inc.; Omaha, NE, USA) and Charge-Coupled Device (CCD) area detector were used to determine the total element content. All analyses were performed in triplicates. The results are expressed as mean  $\pm$  SD<sub>(3)</sub>, where the subscript indicates the number of replicates (three).

### 2.8. Chemicals and Reagents

The chemicals used during the study are: butanal, 3-methyl-; acetic acid, methyl ester; ethyl acetate; butanoic acid, ethyl ester; 2-butanone, 3-hydroxy-; furfural; phenol, 4-ethyl-2-methoxy-. They were obtained from Sigma–Aldrich products, distributed by Merck KGaA, Darmstadt, Germany. The chemicals 1-decanol; n-hexane; nonane; dodecane; tetradecane and hexadecane were obtained from Carlo Erba Reagents, Milano (Italy).

Ultrapure water was obtained using a Milli-Q Plus water system (Millipore, Bedford, MA, USA).

Merck ICP standards (As, B, Ba, S) and multistandards containing 22 elements (Ag, Al, Bi, Ca, Cd, Co, Cr, Cu, Fe, Ga, In, K, Mg, Mn, Na, Ni, P, Pb, Se, Si, Sr, Zn), at different concentrations (10–1000 mg/L), were used to prepare the reference solutions.

All mineral acids and oxidants (HNO<sub>3</sub> and H<sub>2</sub>O<sub>2</sub>) were of the highest purity (Suprapure, Merck; Darmstadt, Germany).

## 3. Results and Discussion

The main aim of this study was to evaluate the chemical composition of defatted grape seeds, and to obtain the preliminary and starting information necessary to make assessments regarding possible future applications. The latter could concern both the food and cosmetic sectors, either as an added natural flavor, or in the context of renewable energy, as a lignocellulosic material. Figure 1 shows the defatted grape seeds (DGS) sample. The color of the matrix is intensely dark because of the thermal roasting process used for the industrial extraction of grape seed oil. The material is powdery, with a particle size < 0.5 mm.



**Figure 1.** The DGS sample.

### 3.1. Proximate Composition

The proximate composition is shown in Table 1. The moisture content of the DGS was 5.96%, whereas the ash content was 2.05%. The residual fat content was very low, confirming the high extraction efficiency of the hot-pressing method. The DGS contained a high amount of crude protein (8.15%). It is important to emphasize that these values can vary depending on the cultivar and genotype of the grape being considered, as well as on the method chosen for fat extraction. As previously mentioned, the DGS sample is obtained from a blend of seeds of different cultivars of origin, as confirmed by the supplier.

**Table 1.** Proximate chemical composition of DGS (%).

<b>Moisture</b>	<b>7.06 ± 0.08</b>
Ash	2.05 ± 0.03
Fats	0.87 ± 0.07
Crude Protein	8.94 ± 0.09
Indigestible total fiber (cellulose, hemicellulose, lignin) [43,44]	~79–80%
C	51.2 ± 0.6
H	6.08 ± 0.13
N	1.43 ± 0.08
S	1.82 ± 0.14
O	37.4 ± 0.4

Data are the mean of 3 replicates ± Standard Deviation (3).

### 3.2. Mineral Content: ICP-OES Determination

Macroelements such as K, Ca, Mg, and P have been determined in the DGS sample, together with some essential microelements and contaminants. Our experimental results are presented in Table 2, with some other pertinent literature data relating only to the integral composition of grape seeds, lacking to our knowledge any further investigation of a similar DGS matrix.

**Table 2.** Elemental composition data of DGS, compared with some different literature data. Adapted with permission from ref. [45] Copyright 2023 Elsevier.

DGS		Literature data [45]	
Element		Niagara (White Grape, Brazil)	Bordo (Red Grape, Brazil)
mg/100 g db			
Ca	19.7 ± 0.7	28.5 ± 0.07	23.03 ± 0.11
K	31.3 ± 1.0	28.32 ± 0.05	39.07 ± 0.05
Mg	10.5 ± 0.6	13.35 ± 0.03	17.21 ± 0.12
P	28.1 ± 1.8	2.13 ± 0.05	3.90 ± 0.10
S	4.38 ± 0.21	2.57 ± 2.35	2.54 ± 0.54
µg/100 g db			
As	0.51 ± 0.06	< LD	< LD
Al	1.95 ± 0.09		
B	11.4 ± 0.5		
Ba	1.32 ± 0.04	10.5 ± 0.6	12.2 ± 0.4
Co	0.19 ± 0.05		
Cr	1.58 ± 0.05		
Cu	14.6 ± 0.6		
Fe	40.2 ± 0.9		

Table 2. Cont.

Element	DGS	Literature data [45]	
		Niagara (White Grape, Brazil)	Bordo (Red Grape, Brazil)
Mn	26.8 ± 0.7	20.0 ± 0.7	32.7 ± 0.9
Na	33.1 ± 1.0		
Ni	0.92 ± 0.08	< LD	< LD
Pb	1.77 ± 0.08	< LD	< LD
Sr	12.9 ± 0.4	22.3 ± 0.2	10.4 ± 0.1
Zn	20.3 ± 0.8	15.6 ± 2.2	16.0 ± 2.4

Data are the mean of 3 replicates ± standard deviation (3).

Despite a thorough literature search, we found useful information only about natural grape seeds, a matrix similar to DGS, to be compared with the values given in Table 2.

The metallic macroelement K is present in greater quantities [ $1 \leq \text{conc (mg/100 g db)}$  without an upper limit], which is in perfect agreement with what has been reported by other authors regarding grape seeds [45].

Similar results have been obtained for other products, such as whole grapes [46], grape juices [47], and wines [48,49], regardless of cultivar and area of origin.

Other metallic macroelements are Ca and Mg, which show concentrations in DGS samples with a mass ratio of about 2:1, their content being  $19.7 \pm 0.7$  and  $10.5 \pm 0.6$  mg/100 g on a dry basis, respectively. These values also satisfactorily agree with those of Gomes et al. [45], although the latter refer to white and red grape seeds. These authors discussed the different contributions of grape skin, pulp, and seeds to the bioaccessibility of micronutrients and main macroelements of two cultivars, representative of red (Bordo) and white (Niagara) grapes from Brazil. Their observations confirmed that Ca and Mg had significantly higher concentrations in the seeds than in the pulp and skin fractions, irrespective of the grape peel color. The significant content of macroelements makes the matrix nutritionally interesting. All these minerals play an important role in human metabolic processes, and each of them must be ingested through the diet to allow for good health. For example, K intake is beneficial in terms of blood pressure and is associated with reduced risk of cardiovascular diseases, incident stroke, and coronary heart disease [50]. There is also evidence that an increased intake of Mg can favorably affect blood pressure, so it can help the prevention and management of hypertension [51,52].

In relation to microelements, Fe, Zn, Cu, Sr, and Mn vary in the range of  $10 \leq \text{conc (}\mu\text{g/100 g db)} \leq 50$  for DGS samples, consistent with the results reported in Gomes et al. [45]. Microdoses of nutrients are essential to ensure the best living conditions for animals and plants, and deficiencies of these elements can seriously affect human health [46]. Similar consideration can apply to Sr, which has always been considered the natural vicarious element of Ca in animals. Despite its low concentration, its occurrence in bone tissue greatly reduces the risk factors for osteoporosis, which tends to appear with aging and in the elderly [53]. Therefore, we can conclude that DGS powder containing modest amounts of macro- and microelements, could be used as a mineral-enriching ingredient in food preparations or supplement formulations. For example, bakery goods enriched with defatted and full-fatted grape seed flours showed higher mineral content, particularly Mg, Ca, K, Zn, and Fe, as reported by some authors [54–56]. We emphasize that grape seed oil extraction does not significantly alter the mineral content of the lignocellulosic residue, i.e., the defatted grape seeds. Therefore, studies concerning full-fatted grape seed flours can also be considered to assess their potential application in the food industry.

Copper at low concentrations is also an essential element for life. Although the European Food Safety Authority (EFSA, Parma, Italy) set the toxicity threshold at 10 mg/day [57], in various environmental contexts it can reach higher values as a result of plant protection treatments. More challenging is the management of elements such as Ni and Pb, which are toxic even at low concentrations and whose presence in DGS can be attributed to some form of soil contamination and circulating water [58]. Currently, European legislation does

not provide maximum levels for nickel as a contaminant in food [59], and the tolerable daily intake (TDI) is 2.8 µg per kg body weight (bw). In contrast, maximum levels for lead and other toxic metals were set by Regulation (EC) No. 1881/2006 [60], and for food supplements, the limit is set at 3.0 mg/kg wet weight. Consequently, both the nickel (0.92 µg/100 g db) and lead (1.77 µg/100 g db) contents in DGS are to be considered safe for human health as their concentrations are significantly below the risk thresholds or set by law.

### 3.3. HS-SPME-GC-MS Analysis

Figure S2 shows the HS-SPME chromatogram obtained from the DGS sample, processed with GC-MS instrumentation immediately after receiving the sample from the Grape Seed Oil Company (Lleida, Spain).

Several compounds were identified based on a combination of some or all of the following criteria: (i) mass spectral data of the libraries supplied with the operating system of the GC-MS and from mass spectra databases; (ii) mass spectra found in the literature; and (iii) mass spectra and retention time of an injected standard. The identified compounds are listed in Table 3. The reproducibility of the results is expressed as standard deviation ( $SD_{(3)}$ ), where the subscript “three” indicates the number of replicates.

**Table 3.** VOC composition of the DGS sample, identified through HS-SPME-GC-MS analysis, grouped by chemical classes. Data are expressed as mean ( $n = 3$ ),  $TIC\ area \times 10^{-5} \pm SD_{(3)}$ .

Compound	LRI	ID #	Aroma	Area $\times 10^{-5}$
<b>Aldehydes</b>				
Acetaldehyde	433	A, B	Pungent, fresh, lifting, fruity, musty	21 $\pm$ 0.4
Propanal, 2-methyl-	550	A, B	Fresh, aldehydic, floral, green	13 $\pm$ 0.3
Butanal, 3-methyl-	654	A, B, C	Ethereal, aldehydic, chocolate, peach, fatty	12 $\pm$ 0.2
Butanal, 2-methyl-	664	A, B	Musty, cocoa, phenolic, coffee, nutty, malty	8.9 $\pm$ 0.1
Pentanal	698	A, B	Fermented, breadly, fruity, berry	10 $\pm$ 0.3
n-Hexanal	806	A, B	Green, fatty, leafy, vegetative, fruity, clean	48 $\pm$ 0.2
Heptanal	902	A, B	Fresh, aldehydic, fatty, green, herbal	4.1 <sup>a</sup>
Benzaldehyde	969	A, B	Almond, fruity, powdery, nutty	1.8 <sup>a</sup>
<b>Alcohols</b>				
Ethanol	461	A, B	Alcoholic	512 $\pm$ 0.4
1-Propanol	546	A, B	Alcoholic, fermented, musty, yeasty	2.2 <sup>a</sup>
<b>Esters</b>				
Formic acid, methyl ester	450	A, B	Fruity, plum, estery	14 $\pm$ 0.3
Formic acid, ethyl ester	509	A, B	Fruity	3.2 <sup>a</sup>
Acetic acid, methyl ester	519	A, B, C	Ethereal, sweet, fruity, winey	102 $\pm$ 0.4
Ethyl acetate	603	A, B, C	Ethereal, fruity, sweet, grape-like, winey	247 $\pm$ 0.2
Butanoic acid, ethyl ester	802	A, B, C	Fruity, juicy, sweet	2.1 $\pm$ 0.1
Butanoic acid, 2-methyl-, ethyl ester	849	A, B	Sharp, sweet, green, apple, fruity	4.1 $\pm$ 0.1
Butanoic acid, 3-methyl-, ethyl ester	853	A, B	Sweet, fruity, sharp, apple, green	5.3 $\pm$ 0.1
1-Butanol, 3-methyl-, acetate	874	A, B	Sweet, fruit	37 $\pm$ 0.3
1-Butanol, 2-methyl-, acetate	878	A, B	Sweet, fruity, ripe	18 $\pm$ 0.2
Hexanoic acid, ethyl ester	977	A, B	Sweet, fruity	5.6 $\pm$ 0.1
Octanoic acid, ethyl ester	1104	A, B	Sweet, waxy, fruity, musty	27 $\pm$ 0.2
Decanoic acid, ethyl ester	1201	A, B	Sweet, waxy, fruity, apple, grape	14 $\pm$ 0.4
<b>Acids</b>				
Formic acid	491	A, B	Pungent, vinegar	1.3 <sup>a</sup>
Acetic acid	584	A, B	Sharp, pungent, sour, vinegar	1046 $\pm$ 0.3
Propanoic acid	671	A, B	Pungent, acidic, cheesy, vinegar	7.9 $\pm$ 0.1
<b>Ketones</b>				
Acetone	488	A, B	Solvent, ethereal, apple, pear	129 $\pm$ 0.4
2-Butanone	585	A, B	Ethereal, diffusive, fruity	16 $\pm$ 0.3
2-Propanone, 1-hydroxy-	621	A, B	Pungent, sweet, caramellic	2.0 <sup>a</sup>
2-Butanone, 3-hydroxy-	710	A, B, C	Sweet, buttery, creamy, dairy, milky, fatty	1.5 <sup>a</sup>
<b>Furan derivatives</b>				
Furan	495	A, B	Ethereal	9.7 $\pm$ 0.1
Furan, 2-methyl-	594	A, B	Ethereal, acetone, chocolate	4.2 <sup>a</sup>
Furfural	842	A, B, C	Sweet, woody, breadly, caramellic, phenolic	39 $\pm$ 0.3
Furan, 2-pentyl-	978	A, B	Fruity, green, earthy, beany, vegetable	2.6 <sup>a</sup>



Table 3. Cont.

Compound	LRI	ID #	Aroma	Area $\times 10^{-5}$
Phenol derivatives				
Phenol	966	A, B		2.2 <sup>a</sup>
Phenol, 2-methoxy-	1053	A, B	Phenolic, smoke, spice, vanilla, woody	3.0 <sup>a</sup>
Phenol, 4-ethyl-2-methoxy-	1160	A, B, C	Spicy, smoky, bacon, phenolic	8.7 $\pm$ 0.1
Terpenes and terpenoids				
$\alpha$ -Pinene	943	A, B	Fresh, camphor, sweet, pine, earthy, woody	6.7 $\pm$ 0.1
$\beta$ -Pinene	985	A, B	Dry, wood, fresh, pine, green, resinous	2.1 <sup>a</sup>
Limonene	1016	A, B	Citrus, herbal, terpene, camphor	3.8 <sup>a</sup>
Eucalyptol	1020	A, B	Eucalyptus, herbal, camphor	4.2 $\pm$ 0.1
Isomenthone	1100	A, B	Minty, cool, peppermint, sweet	1.8 <sup>a</sup>

# The identification is indicated by: (A) mass spectral data of the libraries supplied with the operating system of the GC-MS and from mass spectra databases; (B) mass spectra found in the literature; (C) mass spectra and retention time of an injected standard. <sup>a</sup> SD < 0.05.

As shown in Table 3, a total of 41 compounds were identified in the DGS sample, including aldehydes (8), alcohols (2), ketones (4), acids (3), esters (12), furan derivatives (4), phenol derivatives (3), terpenes and terpenoids (5).

The sample drying process, which is required to extract the residual oil, has contributed to some extent to mobilize and remove the volatile fraction. Some identified analytes probably originate from heat-induced reactions, including the Maillard reaction, carbohydrate and sugar degradation, protein denaturation, and lipid oxidation [61–63]. The Maillard reaction occurs in a wide range of heat-treated foods and is the basis for the generation of their specific flavors [62]. The reaction occurs between a reducing sugar and an amino compound, initially forming a Schiff base, that breaks down in a series of parallel and sequential reactions to form aroma compounds. The Strecker degradation of amino acids is one of the most important reactions leading to final aroma compounds in the Maillard reaction [62,63], particularly the so-called Strecker aldehydes.

Figure 2 can be promptly useful for the interpretation of the results, especially for readers who are not particularly familiar with the typical reaction mechanisms of organic chemistry.

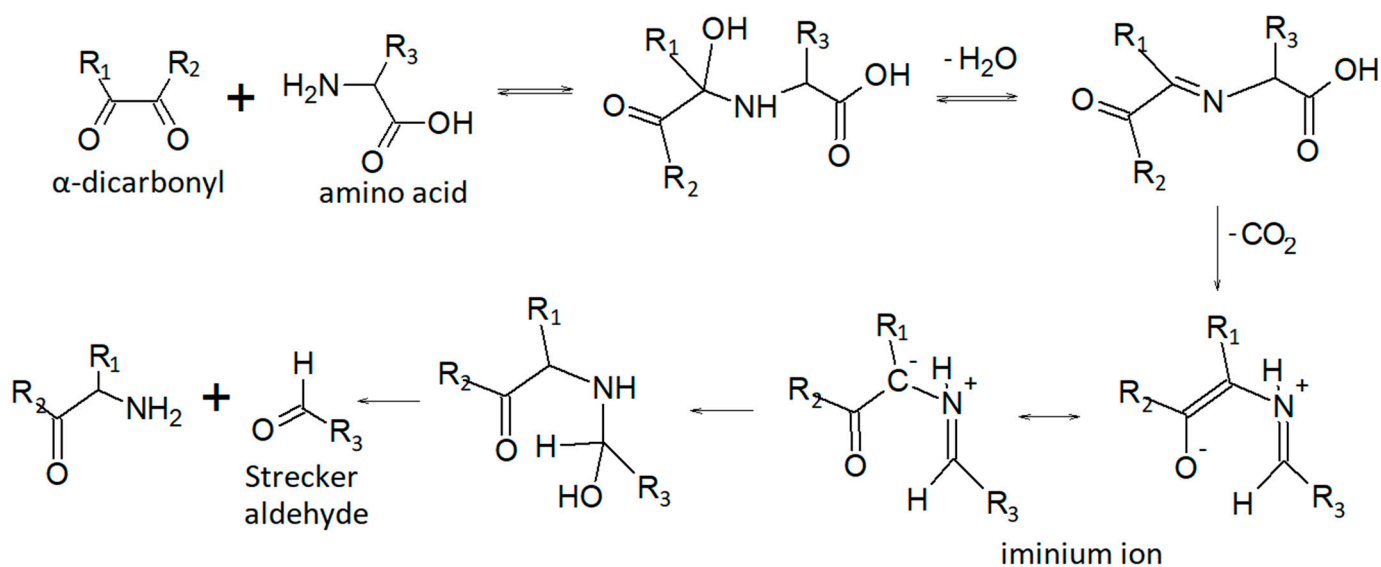


Figure 2. Strecker aldehydes formation pathway [64].

Moreover, since the grape seeds did not undergo any preliminary washing operations, they probably contained some residual molecules from the marc, such as sugars, amino acids, and fatty acids. Furthermore, the marc is subjected to fermentation because of the presence of simple sugars. Therefore, we expected to find some volatile compounds produced during this process.

The volatile compound covering the largest percentage of the total volatiles was acetic acid ( $\text{TIC} = 1045 \times 10^5$ ), followed by ethyl alcohol ( $\text{TIC} = 512 \times 10^5$ ), and ethyl acetate ( $\text{TIC} = 247 \times 10^5$ ).

Aldehydes accounted for 4.9% of the total headspace composition. These molecules are extremely common components of the flavor profile of foods, and many have a low odor threshold [62]. As previously mentioned, aldehydes of different chain lengths can be formed by the Maillard reaction and Strecker degradation, and present different sensory characteristics. In particular, the precursors involved in Strecker degradation are amino acids and diketones derived from the Maillard reaction [63]. Potent flavor compounds 2-Methylpropanal, 2-methylbutanal, and 3-methylbutanal, are the Strecker degradation products of Valine, Isoleucine, and Leucine [65,66], but another proposed pathway is the lipid oxidation of unsaturated fatty acids [63,67]. They were proposed to be responsible for the malty and chocolate-like flavor [63]. Acetaldehyde is an extremely widespread volatile aroma that imparts fruity ether notes. It can be generated from macromolecules of different natures. For example, it can be generated from  $\alpha$ -alanine through Strecker reaction or produced from threonine by lactic acid bacteria [68]. Acetaldehyde is also a precursor of other key volatile aromas such as acetoin. The most abundant aldehyde is n-Hexanal, with a TIC area of  $48 \pm 0.2 \times 10^5$ . It imparts a green bean and cut-grass aroma, as well as the leafy and less ripe notes in many fruit aroma bouquets [62]. In addition, C6 aldehydes, such as hexanal, but also the unsaturated (E)- and (Z)-2-hexenal, are responsible for the green and herbaceous aroma of wines. However, in our sample we only detected n-hexanal: heat treatment probably led to the degradation of these volatile aromas. The high concentration of n-hexanal is probably associated with linoleic acid degradation, the main fatty acid in grape oil. [66,69,70]. Pentanal is also associated with lipid oxidation reactions [66], and, together with hexanal, based on their sensory attributes, these compounds are both responsible for the fresh and slightly green notes of the DGS sample. Benzaldehyde is probably formed from the amino acid L-phenylalanine via the Strecker degradation reaction [66,71]. It is described as having sweet, fruity, nutty, and caramel-like odors [72].

Phenol derivatives (0.58%) can be formed by different reactions: thermal degradation of chlorogenic acids (e.g., ferulic, caffeic, and quinic acids) [63] or lignin, and decarboxylation of phenolic carboxylic acids during roasting [73]. The thermal degradation of lignin through depolymerization or oxidation is one of the main pathways for the formation of phenolic derivatives [72]. This molecule is composed of repeating phenol units with three-carbon side chains [72,74]. In the HS of the GDS sample we identified phenol and two of its derivatives, 2-methoxy-phenol (guaiacol) and 2-methoxy-4-ethyl-phenol (4-ethylguaiacol). They impart a spicy, smoky, sweet, and phenolic aroma [62,72]. Phenol can be generated from the degradation of lignin glycoside during fermentation, whereas 2-methoxy-phenol (guaiacol) is thought to be the thermal degradation product of lignin-related phenolic carboxylic acids [74,75]. Guaiacol is in fact reported to be derived from thermal and oxidative breakdown of ferulic acid which is present in wood lignocelluloses (Figure 3) [75].

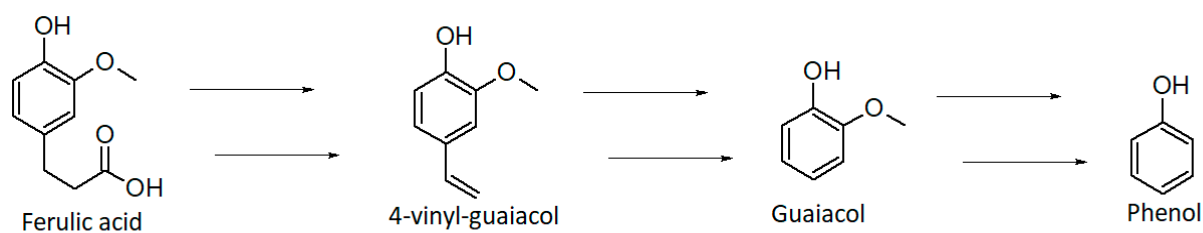


**Figure 3.** Proposed degradation pathway of ferulic acid. Adapted with permission from ref. [75], Copyright 2003 American Chemical Society.

Ketones are well-known by-products of lipid oxidation [70,76], but their formation is also associated with Strecker degradation and Maillard reactions [62]. In particular,

2-butanone is a product of lipid oxidation or degradation [72]. On the other hand, 3-hydroxy-2-butanone is produced during alcoholic fermentation by several microorganisms [72]. It is a characteristic compound of acetification and is present in fermented foods and beverages [72,77]. Moreover, it is one of the most dominant carbonyl compounds in grape pomace [78].

Furan derivatives are mostly formed during Maillard-type reactions [78,79], but can also be produced by other pathways [68]: thermal oxidative degradation of polyunsaturated fatty acids [66], thermal degradation of some amino acids (e.g., serine, threonine, cysteine), breakdown of nucleosides, thermal degradation of carbohydrates [66], ascorbic acid and other organic acids, or carotenes. The Food and Drug Administration (FDA) has reported that a variety of carbohydrate and amino acid mixtures and vitamins, such as ascorbic acid and thiamine, can generate furans in food [68,80]. All these molecules are reasonably present in the marc. Therefore, it is not surprising that furans are present in the HS of the DGS sample. Four furan derivatives have been identified: furan, 2-methylfuran, furfural, and 2-pentylfuran. Furfural and 2-methylfuran are probably formed by sugar dehydration or fragmentation during the Maillard reaction [66,70,79]. Additionally, 2-methylfuran is closely linked to specific amino acids, namely alanine and threonine [79]. Its formation occurs by the recombination of the corresponding Strecker aldehydes in the presence of certain amino acids. On the other hand, 2-Pentylfuran is formed by lipid peroxidation [66]. It has been detected in oxidized soybean oil [81] and olive oil [82]. Therefore, it can be used as a chemical marker of rancidity [67]. Furan has received considerable attention due to its classification as “possibly carcinogenic to humans” [68,83]. It is found in relatively high amounts in foods that have undergone heat treatment. Its formation is associated with lipid peroxidation, through cyclization and formation of the intermediate 2,5-dihydro-2-furanol from 4-hydroxy-2-butenal and subsequent dehydration as proposed in Figure 4. However, some studies associated it with other pathways, including amino acid degradation [68,84], carbohydrate degradation [68,79], and ascorbic acid oxidation [68].

Only three acids were detected in the DGS sample. Among them, acetic acid content was the highest in the entire chromatogram profile. It can be formed during the intermediate stage of the Maillard reaction, the breakdown and dehydration of the sugar moieties [62]. Moreover, acetic acid can be formed by both aerobic and anaerobic fermentation by specific bacteria [85]. Under aerobic conditions, glucose is converted to ethanol, which is subsequently converted to acetic acid. We can therefore affirm that the very high content of acetic acid is probably due to a combination of both thermal and fermentation processes, the latter carried out by bacteria present in the marc. Furthermore, propanoic acid is considered a by-product of yeast protein metabolism [72]. Since ethyl esters are derived from the esterification of free fatty acids and ethanol, their corresponding fatty acids are expected to be present [72]. However, the results indicated that the latter was almost absent, despite the presence of the corresponding esters. This could be an indication of strong esterification during the fermentation process [86].

Twelve esters were detected in the sample's HS. Ester formation is associated with lipid oxidation of polyunsaturated fatty acids [62], which are abundant in grape seeds [73]. Moreover, several studies associate their formation with alcoholic fermentation processes, which are linked to yeast metabolism [86–89]. Short-chain esters are among the most important VOCs in a wide range of food samples, such as cheese, wine, and apples [62,76,86–89]. Their contribution to the overall aroma is considered positive, but if present at high concentrations, they become off-flavors, as they impart strong fruity and fermented notes. In general, esters impart fruity notes with sensory descriptions ranging from fruity and solvent-like, banana and pear-like, rose- and honey-like, or apple-like and sweet. Ethyl esters are among the main components of fruit aroma. The longer the carbon chain, the more soapy, cheesy, and waxy the aroma of ethyl esters becomes. Moreover, ethyl esters and acetates are the two main odor-active esters of wine. We detected seven ethyl esters and three acetates and, among them, ethyl acetate was the most abundant. Together with isoamyl acetate (1-butanol, 3-methyl-, acetate), the latter is the most important ester in

wine [88]. The ester composition of wine HS is generally more complex and is characterized by a large number of volatile species [86,87,89]. Despite this, we observed that our DGS sample presented olfactory notes characteristic of wine. This experimental observation is probably due to the fermentation processes occurring in the marc.

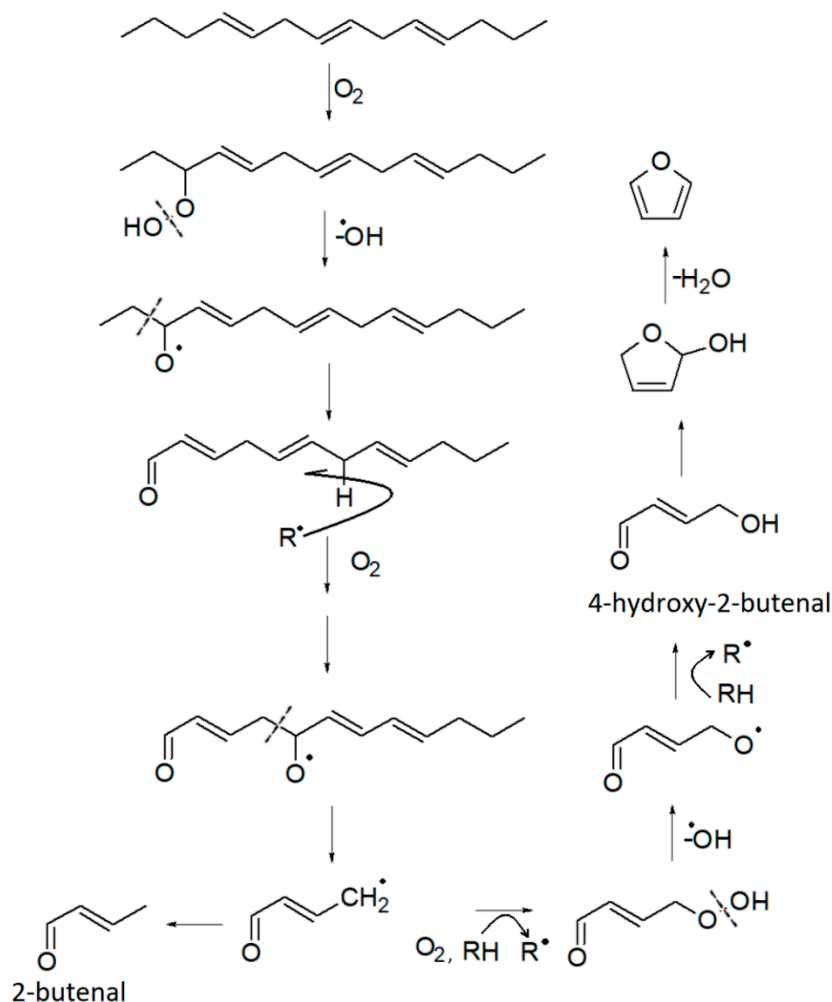


**Figure 4.** Proposed formation pathway of furan and some other VOCs, starting from a triene hydrocarbon. Adapted with permission from ref. [68], Copyright 2004 American Chemical Society.

Terpenes and terpenoids are the main components of essential oils and constitute the specific aroma profiles of many fruits, herbs, and spices [62]. They cover 34,000 to 50,000 different molecules, but mainly monoterpenes and sesquiterpenes have been identified as flavor contributors in fruits and vegetables. In our DGS sample we have detected only five species belonging to this class, all with a very low TIC area. Irregular terpenes (norisoprenoids) play an important role in wine aroma, and a lot of research has been performed on this compound class in the wine context [90–92]. They are produced by breakdown of the grapes' carotenoids, which have been detected not only in the fresh fruit, but also in the must [91]. Nevertheless, norisoprenoids were not identified in the DGS sample. Their absence can be attributed to the heat treatment of the matrix, which may have led to the loss of these volatile analytes.

Table 4 summarizes the results obtained from the HS-SPME-GC-MS analysis of the DGS sample, collected in a comparative form based on the classes of compounds identified.

**Table 4.** Compound classes identified in the HS-SPME-GC-MS analysis of the DGS sample.

Compound Class	Mean * $\pm$ SD <sub>(3)</sub>
Aldehydes	4.51 $\pm$ 0.05
Alcohols	21.35 $\pm$ 0.02
Esters	20.00 $\pm$ 0.12
Acids	43.82 $\pm$ 0.02
Ketones	6.21 $\pm$ 0.03
Furan derivatives	2.32 $\pm$ 0.02
Phenol derivatives	0.58 $\pm$ 0.01
Terpenes and Terpenoids	0.77 $\pm$ 0.01

Data are expressed as mean % of each class to the total normalized peak areas on the basis of the sum of the TIC area. \* Mean of three replicates of the chromatograms  $\pm$  standard deviation SD<sub>(3)</sub>.

The most abundant molecular class is acids, whose main contribution is acetic acid, followed by alcohols and esters. The origin of the analytes belonging to these classes can be attributed to the combination of both the thermal and fermentation processes. This would explain the greater abundance compared to the volatiles belonging to the classes of aldehydes, ketones, furan, and phenolic derivatives, whose origin is mainly heat-induced reactions starting from carbohydrates, lipids, and amino acids. Finally, the class of terpenes and terpenoids was not particularly abundant and significant, even though we expected characteristic analytes of the marc.

HS-SPME-GC-MS analysis results showed a complex aroma profile, which provides the sample with a distinctive and unique flavor. The inclusion of DGS in food preparations can modify their sensory characteristics, as shown in studies involving bakery goods enriched with grape seed flour [54–56,93–95]. In some preparations, such as cereal bars, the addition of DGS increased consumer acceptability compared with the control product [94]. In others, once a certain added quantity is exceeded, the acceptability decreases [93–95]. However, the authors obtained good sensory acceptance by adjusting the amount of sample added, while retaining the beneficial health effects in each case.

### 3.4. TGA-MS-EGA Analysis

The compositional complexity of a biomass leads to greater complexity in the thermogravimetric profile. As previously pointed out, the DGS sample consists mainly of polysaccharides, such as cellulosic constituents, as well as a moderate protein content (8.94%). Therefore, TGA-MS-EGA provides information regarding the various degradative processes involving all the constituents, i.e., processes that also occur simultaneously in partial or total overlap in specific temperature ranges identifiable in the thermogram. When several degradative reactions occur simultaneously, the thermogram profile is the sum of the various contributions in the superimposed form. In these cases, the deconvolution of the signals is not particularly easy and effective, especially if the different processes lead to the formation of the same reaction products, such as H<sub>2</sub>O, CO, and CO<sub>2</sub>. For effective interpretation of thermograms, the temperature range is generally divided into intervals of different size and characteristic.

From the values reported in Table 1, the total organic mass of the DGS sample was around ~90–91%, including the protein content (~8.9%). The literature [90,96] shows that starches and simple sugars are generally present at trace levels in this material. The same is true for other compounds of high biological value such as polyphenols and tannins, but with modest and poorly significant contributions to the total organic mass. It follows that the residual mass with fixed carbon (~82%) consists of the main indigestible fractions of cellulose, hemicellulose, and lignin.

The result of the TGA, together with its first derivative (DTG), runs in inert atmosphere (He) as shown in Figure 5, while the related quantitative considerations are summarized in Table 5.



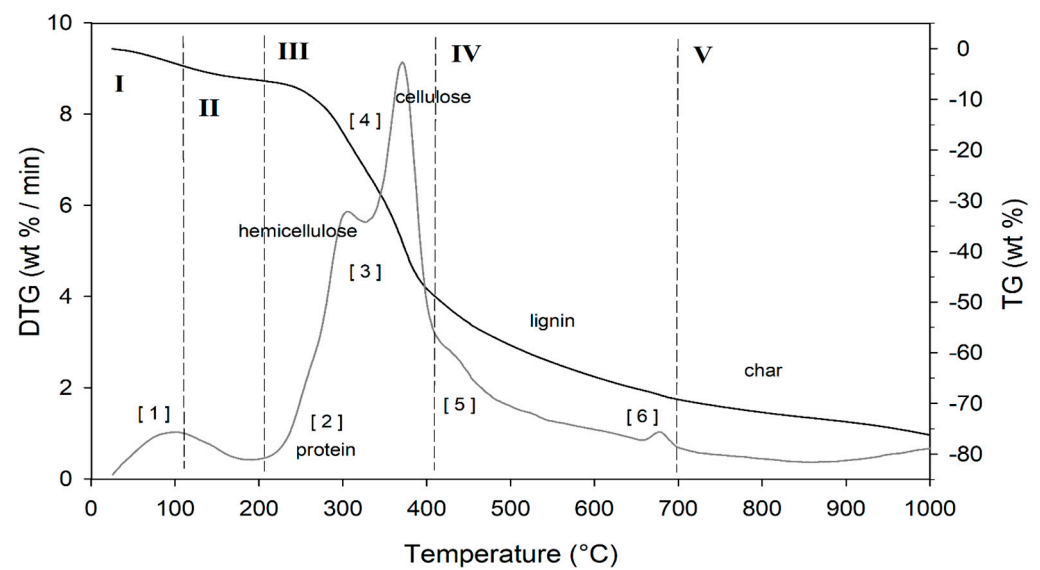


**Figure 5.** TG (black line) and DTG (grey line) curves of DGS sample at heating rate of 20 °C/min in He atmosphere. Vertical dashed red lines delimit the five thermal regions (I–V) described in the text. For the meaning of the numbers in parentheses, see Table 5.

**Table 5.** Representative values of TGA/DTG profiles of Figure 5, obtained in inert atmosphere (He).

Region	Thermal Step	T <sub>o</sub>	T <sub>m</sub>	T <sub>c</sub>	Δm%	Thermally Activated Processes
I	1	30	99.4	120	−3.5	Removal of moisture and VOCs up to 105–120 °C
II	1	120	—	211.3	−3.1	Removal of bound water, NH <sub>3</sub> from protein denaturation, low-boiling VOCs, loss of CO and CO <sub>2</sub> , and caramelization of sugars
	2	211.3	—	263.3	−3.2	Shoulder related to protein degradation
III	3	263.3	299.0	316.2	−12.8	Removal of reaction water, NH <sub>3</sub> , low-boiling VOCs, and SVOCs, decarboxylation of acids with CO <sub>2</sub> loss, degradation of polysaccharides, plasticization, and pseudo-vitrification of the sample
	4	316.2	365.9	413.4	−26.7	Fat degradation, removal of hydrocarbons, water of constitution, CO, and CO <sub>2</sub> , and volatilization of other metabolites
	5	413.4	434.5	463.6	−11.2	Removal of reaction water, CO <sub>2</sub> and other metabolites
IV		463.6	—	650	−9.4	Weak reactions related to slow volatilization of CO <sub>2</sub> , carbon residues and other molecules
	6	650	675	695.5	−2.1	Removal of reaction water, CO and CO <sub>2</sub> , and other metabolites
V		695.5	—	1000	−7.3	Volatilization of carbon residues, probably C <sub>20</sub> –C <sub>40</sub> fragments
Residual ashes at 1000 °C						Inorganic compounds and carbon residue

T<sub>o</sub> = onset temperature (beginning of thermal step processes); T<sub>m</sub> = maximum temperature for the largest mass loss rate; T<sub>c</sub> = conclusion temperature (end of thermal step processes).

The thermogram domain is divided into five regions, each representing the behavior of the matrix in relation to some specific processes. Region I, which covers the temperature range up to  $\sim 120$  °C, is attributed to the drying phase (moisture removal) and simultaneous thermal removal of particularly volatile organic compounds, which constitute the characteristic aroma profile of the matrix ( $-\Delta m\% = 3.5\%$ ). Within this region, other thermally activated processes occur without loss of mass, such as the denaturation of proteins by unfolding [97,98]. Region II, which covers the temperature range from  $\sim 120$  °C to  $\sim 211$  °C, represents the mass loss related to bound water, i.e., the water typically retained by the inorganic fraction, such as the crystallization water of mineral salts. In this region, semi-volatile compounds with medium-low vapor pressure (SVOCs), present in the initial matrix or formed during the heating phase, are completely removed ( $\Delta m\% = -3.1\%$ ). Around  $160$  °C the removal of structural water begins, which is formed by condensation reactions of the  $-\text{OH}$  groups present mainly in simple non-cellulosic carbohydrates [99]. The formation and removal of reaction waters traverse the entire thermogram, up to and including region IV (Figure 5). Furthermore, near the upper temperature limit ( $\sim 180$  °C), free amino acids begin to undergo thermal degradation processes [100], while proteins persist up to  $\sim 200$ – $220$  °C. Thus, the processes occurring in this region suggest that the chemical structure of the biomass begins to destabilize, partly depolymerize, and plasticize. Region III, subtended in the temperature range from  $\sim 211$  °C to  $\sim 413$  °C, represents the main pyrolysis window where structural decay reactions of proteins ( $\sim 240$  °C), hemicellulose ( $\sim 300$  °C) [101,102], and cellulose ( $\sim 370$  °C) [97,102,103] are observed. The mass loss in this region is approximately  $\Delta m\% = -43.9\%$ .

Region IV begins at  $\sim 413$  °C and extends up to  $\sim 695$  °C. In this thermal window, the gradual mass decrease ( $\Delta m\% = -28.2\%$ ) is mainly due to the slow pyrolysis of the lignin fraction [104], which is associated with sample vitrification and volatilization of carbon microparticles. The small thermal event near  $700$  °C can be attributed to the thermal decomposition of carbonaceous matter (biochar), mostly related to the hemicellulosic fraction [105], even though lignin components may contribute to its formation [106]. However, from the evolution profiles of the analytes with  $m/z = 18$  and  $m/z = 44$  (Figure 6), it is observed that this thermal reaction corresponds to the formation and volatilization of  $\text{CO}_2$ . The explanation requires some further considerations, because two types of processes can satisfy the experimental evidence:

- i. a metal carbonate  $\text{MCO}_3$  can decompose into  $\text{M}_x\text{O}_y + \text{CO}_2$ ;
- ii. a metal oxide  $\text{M}_x^{n+}\text{O}_y$  can be reduced to a lower oxidation number  $\text{M}_x^{m+}\text{O}_y$  ( $n > m$ ) in the presence of C residues and release  $\text{CO}_2$ .

To the best of our knowledge, the literature does not provide further information on these questions.

In region V, above  $\sim 700$  °C, to the final temperature ( $1000$  °C), the last residues of biomass degradation can be observed. This is the typical carbon pyrolysis window with the thermal decomposition of low volatile matter ( $\Delta m\% = -7.3\%$ ) such as carbon fragments  $\text{C}_{20}$ – $\text{C}_{40}$ , in presence of mineral ashes.

Lastly, the release of  $\text{NO}$  ( $m/z = 30$ ) and  $\text{SO}_2$  ( $m/z = 64$ ) fragments was verified, but their signal-to-noise ratio was extremely low, and did not give significant results.

The TGA/DTG profile of DGS is typical of lignocellulosic raw materials, highlighting the content of cellulose, hemicellulose, and lignin, which are classified as non-soluble dietary fibers (IDF) [107]. This observation was confirmed by proximate composition analysis (Section 3.1, Figure 1). IDF provide several health benefits [108–110], as their intake is associated with the prevention and treatment of cardiovascular diseases [108–110], diabetes [110], and colon cancer [108]. Moreover, their addition affects the sensory characteristics of food products, mainly their texture [107]. IDF increase firmness and provide a high fat absorption capacity; therefore, they can be exploited to achieve desired functional properties [111]. Some applications of IDF involve bakery goods [112], such as biscuits, bread, or snacks, cooked meat products [113], sauces, desserts, and yogurts, where they act as bulking agents while reducing calorie content [111]. For example, the addition of IDF

sources to beef burgers [113] leads to fat reduction without modifying the sensory characteristics. A further example concerns “light” chocolate production with added IDF sources, which results in a firm, smooth texture, and easy removal from the mold [111]. On the other hand, in bakery products, IDF sources replace part of the flour, resulting in significant nutritional benefits by increasing fiber content and reducing calorie intake [112]. IDF from cereals are more frequently exploited than those from fruit processing, but the latter have a higher bioactive compound content and can therefore exert higher health-promoting effects than dietary fiber itself [109].

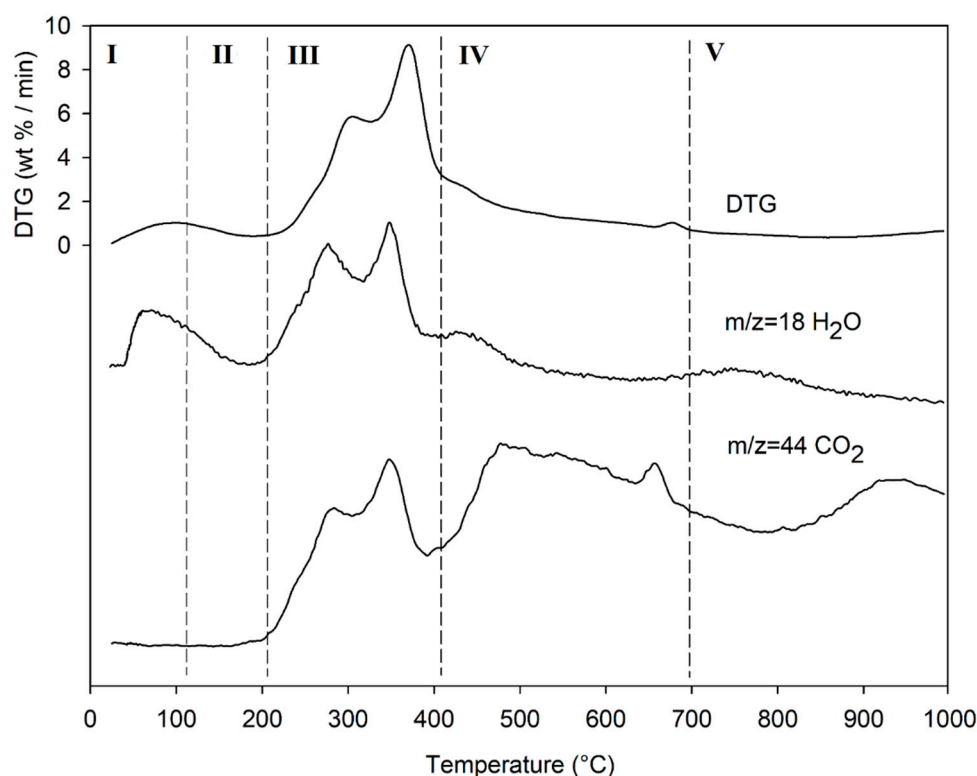


**Figure 6.** Evolution trend of H<sub>2</sub>O and CO<sub>2</sub> during the heating of DGS sample; for ease of comparison, the DTG curve is also shown. Intensity of  $m/z$  is in arbitrary units. Region I–V = thermal regions identified in the thermogram of Figure 5 and explained in Table 5.

#### 4. Conclusions

Some investigation about the DGS composition showed that this biomass is not at all a waste by-product, to be eliminated from the environment as a compost or as a fuel to produce bioenergy. The latter applications certainly respect the circular economy principles. However, there may be alternative applications and methods for valorization. DGS may be a very useful dietary supplement, as it is a precious source of many different nutrients, capable of improving human health and promoting animal wellness. Proximal analysis revealed a significant protein content, whereas the residual lipid content after oil extraction was extremely low. This evidence suggests a great potential as a low-fat and high-protein ingredient for healthy food and feed formulations. In addition, the DGS is a great source of metallic macroelements and essential microelements. The presence of very few toxic heavy metals is not to be considered unsafe for human health, given their low concentration and as suggested by international regulations. This complex matrix showed an aroma profile extremely peculiar and characteristic, defined by molecules originating from thermally activated reactions (e.g., Maillard) and fermentation processes.

In conclusion, the use of DGS in the food chain enhances its beneficial effects on human health and simultaneously reduces the environmental impact of the wine sector, producing a large quantity of waste by-products. DGS powder can be used as a nutritionally and

functionally enriching food, for example, in bakery goods, and feed, thanks to its high content of dietary fibers, minerals, proteins, antioxidants, polyphenols, and low lipid content. At the same time, it can impart specific and peculiar aromatic notes to food and feed preparations, thus improving their sensory characteristics.

**Supplementary Materials:** The following supporting information can be downloaded at: <https://www.mdpi.com/article/10.3390/life13020326/s1>, Figure S1: The wines of Italy: Randi Group supply area; Figure S2: Total ion current chromatogram of VOCs from the DGS sample, obtained using HS-SPME-GC-MS.

**Author Contributions:** Conceptualization, V.D. and F.R.; methodology, V.D. and D.M.; software, V.D. and F.R.; validation, V.D. and D.M.; formal analysis, A.M. and V.D.; investigation, V.D., D.M. and A.M.; resources, V.D. and A.M.; data curation, V.D. and F.R.; writing—original draft preparation, V.D. and L.T.; writing—review and editing, V.D. and D.M.; visualization, V.D. and D.M.; supervision, V.D. and F.R.; project administration, L.T. and V.D.; funding acquisition, A.M., L.T. and V.D. All authors have read and agreed to the published version of the manuscript.

**Funding:** This research was funded by Mineral Reactivity, a Key to Understand Large-Scale Processes: from Rock Forming Environments to Solid Waste Recovering/Lithification, grant number PRIN2017L83S77.

**Institutional Review Board Statement:** Not applicable.

**Informed Consent Statement:** Not applicable.

**Data Availability Statement:** Data is contained within the article.

**Acknowledgments:** It is a pleasure to gratefully thank Giovanni Randi s.p.a. (Randi Group, Faenza, Italy) for providing us the defatted grape seeds (DGS) material used for experiments [<https://www.randi-group.com/it/randi-group/>, accessed on 15 November 2022].

**Conflicts of Interest:** The authors declare no conflict of interest.

## References

1. Torres-Leon, C.; Ramirez-Guzman, N.; Lonzone-Hernandez, L.; Martinez-Medina, G.A.; Diaz-Herrera, R.; Navarro-Macias, V.; Alvarez-Perez, O.B.; Picazo, B.; Villareal-Vazquez, M.; Ascacio-Valdes, J.; et al. Food Waste and Byproducts: An Opportunity to Minimize Malnutrition and Hunger in Developing Countries. *Front. Sustain. Food Syst.* **2018**, *2*, 1–17. [[CrossRef](#)]
2. Maletti, L.; D'Eusario, V.; Durante, C.; Marchetti, A.; Pincelli, L.; Tassi, L. Comparative Analysis of VOCs from Winter Melon Pomace Fibers before and after Bleaching Treatment with H<sub>2</sub>O<sub>2</sub>. *Molecules* **2022**, *27*, 2336. [[CrossRef](#)]
3. Hamam, M.; Chinnici, G.; Di Vita, G.; Pappalardo, G.; Pecorino, B.; Maesano, G.; D'Amico, M. Circular Economy Models in Agro-Food Systems: A Review. *Sustainability* **2021**, *13*, 3453. [[CrossRef](#)]
4. UN General Assembly. Transforming our world: The 2030 Agenda for Sustainable Development. 2015. Available online: <https://www.refworld.org/docid/57b6e3e44.html> (accessed on 3 November 2022).
5. Ayala, J.; Vega, V.; Rosas, C.; Palafox, H.; Villa, J.; Siddiqui, W. Agro-industrial potential of exotic fruit byproducts as a source of food additives. *Food Res. Int.* **2011**, *44*, 1866–1874. [[CrossRef](#)]
6. Bordiga, M.; Travaglia, F.; Locatelli, M. Valorisation of grape pomace: An approach that is increasingly reaching its maturity—A review. *Int. J. Food Sci. Technol.* **2019**, *54*, 933–942. [[CrossRef](#)]
7. Saykova, I.; Tylkowski, B.; Popovici, C.; Peev, G. Extraction of phenolic and flavonoid compounds from solid wastes of grape seed oil production by cold pressing. *J. Chem. Technol. Metall.* **2018**, *53*, 177–190.
8. Ferrari, V.; Taffarel, S.R.; Espinosa-Fuentes, E.; Oliveira, M.L.S.K.; Saikia, B.K.; Oliveira, L.F.S. Chemical evaluation of by-products of the grape industry as potential agricultural fertilizers. *J. Clean. Prod.* **2019**, *208*, 297–306. [[CrossRef](#)]
9. Ferrer, J.; Páez, G.; Mármol, Z.; Ramones, E.; Chandler, C.; Marín, M.; Ferrer, A. Agronomic use of biotechnologically processed grape wastes. *Bioresour. Technol.* **2001**, *76*, 39–44. [[CrossRef](#)]
10. Grosu, I.A.; Pistol, G.C.; Taranu, I.; Marin, D.E. The Impact of Dietary Grape Seed Meal on Healthy and Aflatoxin B1 Afflicted Microbiota of Pigs after Weaning. *Toxins* **2019**, *11*, 25. [[CrossRef](#)]
11. Garcia, J.; Nicodemus, N.; Carabano, R.; De Blass, J.C. Effect of inclusion of defatted grape seed meal in the diet on digestion and performance of growing rabbits. *J. Anim. Sci.* **2002**, *80*, 162–170. [[CrossRef](#)]
12. Zúñiga-Muro, N.M.; Bonilla-Petriciolet, A.; Mendoza-Castillo, D.I.; Reynel-Ávila, H.E.; Duran-Valle, C.J.; Ghalla, H.; Sellaoui, L. Recovery of grape waste for the preparation of adsorbents for water treatment: Mercury removal. *J. Environ. Chem. Eng.* **2020**, *8*, 103738. [[CrossRef](#)]

13. Al Juhaimi, F.; Gecgel, U.; Gulcu, M.; Ozcan, M.M. Bioactive Properties, Fatty Acid Composition and Mineral Contents of Grape Seed and Oils. *S. Afr. J. Enol. Vitic.* **2017**, *38*, 103–108. [\[CrossRef\]](#)
14. Gitea, M.A.; Bungau, S.G.; Gitea, D.; Pasca, B.M.; Purza, A.L.; Radu, A.-F. Evaluation of the Phytochemistry–Therapeutic Activity Relationship for Grape Seeds Oil. *Life* **2023**, *13*, 178. [\[CrossRef\]](#)
15. Baroi, A.M.; Popitui, M.; Fierascu, I.; Sărdărescu, I.-D.; Fierascu, R.C. Grapevine Wastes: A Rich Source of Antioxidants and Other Biologically Active Compounds. *Antioxidants* **2022**, *11*, 393. [\[CrossRef\]](#)
16. Mandic, A.I.; Dilas, S.M.; Cetkovic, G.S.; Canadanovic-Brunet, J.M.; Tumbas, V.T. Polyphenolic Composition and Antioxidant Activities of Grape Seed Extract. *Int. J. Food Prop.* **2008**, *11*, 713–726. [\[CrossRef\]](#)
17. Kapcsandi, V.; Lakatos, E.H.; Sik, B.; Linka, L.A.; Szekelyhidi, R. Characterization of fatty acid, antioxidant, and polyphenol content of grape seed oil from different *Vitis vinifera* L. varieties. *OCL* **2021**, *28*, 30. [\[CrossRef\]](#)
18. Marin, D.E.; Bulgaru, C.V.; Anghel, C.A.; Pistol, G.C.; Dore, M.I.; Palade, M.L.; Taranu, I. Grape Seed Waste Counteracts Aflatoxin B1 Toxicity in Piglet Mesenteric Lymph Nodes. *Toxins* **2020**, *12*, 800. [\[CrossRef\]](#)
19. Di Stefano, V.; Buzzanca, C.; Melilli, M.G.; Indelicato, S.; Mauro, M.; Vazzana, M.; Arizza, V.; Lucarini, M.; Durazzo, A.; Bongiorno, D. Polyphenol Characterization and Antioxidant Activity of Grape Seeds and Skins from Sicily: A Preliminary Study. *Sustainability* **2022**, *14*, 6702. [\[CrossRef\]](#)
20. Yilmaz, Y.; Toledo, R.T. Health aspects of functional grape seed constituents. *Trends Food Sci. Technol.* **2004**, *15*, 422–433. [\[CrossRef\]](#)
21. Kaur, M.; Agarwal, C.; Agarwal, R. Anticancer and Cancer Chemopreventive Potential of Grape Seed Extract and Other Grape-Based Products. *J. Nutr.* **2009**, *139*, 1806S–1812S. [\[CrossRef\]](#)
22. Shi, J.; Yu, J.; Pohorly, J.; Young, J.C.; Bryan, M.; Wu, Y. Optimization of the extraction of polyphenols from grape seed meal by aqueous ethanol solution. *Food Agric. Environ.* **2003**, *1*, 42–47.
23. De Souza, R.d.C.; Machado, B.A.S.; de Barreto, G.A.; Leal, I.L.; Anjos, J.P.D.; Umsza-Guez, M.A. Effect of Experimental Parameters on the Extraction of Grape Seed Oil Obtained by Low Pressure and Supercritical Fluid Extraction. *Molecules* **2020**, *25*, 1634. [\[CrossRef\]](#)
24. Salem, Y.; Rajha, H.N.; van den Broek, L.A.M.; Safi, C.; Togtema, A.; Manconi, M.; Manca, M.L.; Debs, E.; Hobaiika, Z.; Maroun, R.G.; et al. Multi-Step Biomass Fractionation of Grape Seeds from Pomace, a Zero-Waste Approach. *Plants* **2022**, *11*, 2831. [\[CrossRef\]](#)
25. Makris, D.P.; Boskou, G.; Andrikopoulos, N.K. Polyphenolic content and in vitro antioxidant characteristics of wine industry and other agri-food solid waste extracts. *J. Food Compos. Anal.* **2007**, *20*, 125–132. [\[CrossRef\]](#)
26. Druaux, C.; Voilley, A. Effect of food composition and microstructure on volatile flavour release. *Trends Food Sci. Technol.* **1997**, *8*, 364–368. [\[CrossRef\]](#)
27. Guenter, M. The Flavour and Fragrance Industry, Past Present, and Future. In *Flavours and Fragrances, Chemistry, Bioprocessing and Sustainability*, 1st ed.; Berger, R.G., Ed.; Springer: Berlin/Heidelberg, Germany; New York, NY, USA, 2007; Volume 1, Chapter 1, pp. 1–14.
28. Harmon, A.D. Solid-phase microextraction for the analysis of flavors. In *Techniques for Analyzing Food Aroma*, 1st ed.; Marsili, R., Ed.; Marcel Decker, Inc.: New York, NY, USA, 1997; pp. 81–112.
29. Vas, G.; Vékey, K. Solid-phase microextraction: A powerful sample preparation tool prior to mass spectrometric analysis. *J. Mass Spectrom.* **2004**, *39*, 233–254. [\[CrossRef\]](#)
30. Ozsin, G.; Putun, A.E. Kinetics and evolved gas analysis for pyrolysis of food processing wastes using TGA/MS/FT-IR. *Waste Manag.* **2017**, *64*, 315–326. [\[CrossRef\]](#)
31. Parparita, E.; Nistor, M.T.; Popescu, M.; Vasile, C. TG/FT-IR/MS study on thermal decomposition of polypropylene/biomass composites. *Polym. Degrad. Stab.* **2014**, *109*, 13–20. [\[CrossRef\]](#)
32. Brebu, M.; Yanik, J.; Uysal, T.; Vasile, C. Thermal and Catalytic Degradation of Grape Seeds/Polyethylene Waste Mixture. *Cellul. Chem. Technol.* **2014**, *48*, 665–674.
33. Sanchez-Silva, L.; Lopez-Gonzales, D.; Villasenor, J.; Sanchez, P.; Valverde, J.L. Thermogravimetric-mass spectrometric analysis of lignocellulosic and marine biomass pyrolysis. *Bioresour. Technol.* **2012**, *109*, 163–172. [\[CrossRef\]](#)
34. Rombaut, N.; Savoie, R.; Thomasset, B.; Belliard, T.; Castello, J.; Van Hecke, E.; Lanoiselle, J.L. Grape seed oil extraction: Interest of supercritical fluid extraction and gas-assisted mechanical extraction for enhancing polyphenol co-extraction in oil. *C. R. Chim.* **2014**, *17*, 284–292. [\[CrossRef\]](#)
35. Rombaut, N.; Savoie, R.; Thomasset, B.; Castello, J.; Van Hecke, E.; Lanoiselle, J.L. Optimization of oil yield and oil total phenolic content during grape seed cold screw pressing. *Ind. Crops Prod.* **2015**, *63*, 26–33. [\[CrossRef\]](#)
36. Coelho, J.; Filipe, R.M.; Robalo, M.P.; Stateva, R.P. Recovering value from organic waste materials: Supercritical fluid extraction of oil from industrial grape seeds. *J. Supercrit. Fluids* **2018**, *141*, 68–77. [\[CrossRef\]](#)
37. Bravi, M.; Spinoglio, F.; Verdone, N.; Adami, M.; Aliboni, A.; D'Andrea, A.; De Santis, A.; Ferri, D. Improving the extraction of  $\alpha$ -tocopherol-enriched oil from grape seeds by supercritical CO<sub>2</sub>. Optimisation of the extraction conditions. *J. Food Eng.* **2007**, *78*, 488–493. [\[CrossRef\]](#)
38. Shinangawa, F.B.; Santana, F.C.D.; Torres, L.R.O.; Mancinifiliho, J. Grape seed oil: A potential functional food? *Food Sci. Technol.* **2015**, *35*, 399–406. [\[CrossRef\]](#)



39. Chikwanha, O.C.; Raffrenato, E.; Muchenje, V.; Musarurwa, H.T.; Mapiye, C. Varietal Differences in Nutrient, Amino Acid and Mineral Composition and in Vitro Rumen Digestibility of Grape (*Vitis Vinifera*) Pomace from the Cape Winelands Vineyards in South Africa and Impact of Preservation Techniques. *Ind. Crops Prod.* **2018**, *118*, 30–37. [\[CrossRef\]](#)
40. Sah, R.N.; Miller, R.O. Spontaneous Reaction for Acid Dissolution of Biological Tissues in Closed Vessels. *Anal. Chem.* **1992**, *64*, 230–233. [\[CrossRef\]](#)
41. Durante, C.; Cocchi, M.; Lancellotti, L.; Maletti, L.; Marchetti, A.; Roncaglia, F.; Sighinolfi, S.; Tassi, L. Analytical Concentrations of Some Elements in Seeds and Crude Extracts from *Aesculus Hippocastanum*, by ICP-OES Technique. *Agronomy* **2020**, *11*, 47. [\[CrossRef\]](#)
42. Maletti, L.; D'Eusano, V.; Lancellotti, L.; Marchetti, A.; Pincelli, L.; Strani, L.; Tassi, L. Candying Process for Enhancing Pre-Waste Watermelon Rinds to Increase Food Sustainability. *Future Foods* **2022**, *6*, 100182. [\[CrossRef\]](#)
43. Goñi, I.; Martín, N.; Saura-Calixto, F. In Vitro Digestibility and Intestinal Fermentation of Grape Seed and Peel. *Food Chem.* **2005**, *90*, 281–286. [\[CrossRef\]](#)
44. Bordiga, M. *Valorization of Wine Making by-Products*; CRC Press: Boca Raton, FL, USA, 2016.
45. Gomes, T.M.; Toaldo, I.M.; Haas, I.C.d.S.; Burin, V.M.; Caliari, V.; Luna, A.S.; de Gois, J.S.; Bordignon-Luiz, M.T. Differential Contribution of Grape Peel, Pulp, and Seed to Bioaccessibility of Micronutrients and Major Polyphenolic Compounds of Red and White Grapes through Simulated Human Digestion. *J. Funct. Foods* **2019**, *52*, 699–708. [\[CrossRef\]](#)
46. Acuña-Avila, P.E.; Vásquez-Murrieta, M.S.; Franco Hernández, M.O.; del López-Cortéz, M.S. Relationship between the Elemental Composition of Grapeyards and Bioactive Compounds in the Cabernet Sauvignon Grapes *Vitis Vinifera* Harvested in Mexico. *Food Chem.* **2016**, *203*, 79–85. [\[CrossRef\]](#)
47. Toaldo, I.M.; Fogolari, O.; Pimentel, G.C.; de Gois, J.S.; Borges, D.L.G.; Caliari, V.; Bordignon-Luiz, M. Effect of Grape Seeds on the Polyphenol Bioactive Content and Elemental Composition by ICP-MS of Grape Juices from *Vitis Labrusca*, L. Lebonson. *Wiss. Technol.* **2013**, *53*, 1–8. [\[CrossRef\]](#)
48. Vievard, J.; Amoikon, T.L.-S.; Coulibaly, N.A.; Devouge-Boyer, C.; Arellano-Sánchez, M.G.; Aké, M.F.D.; Djeni, N.T.; Mignot, M. Extraction and Quantification of Pesticides and Metals in Palm Wines by HS-SPME/GC-MS and ICP-AES/MS. *Food Chem.* **2022**, *393*, 133352. [\[CrossRef\]](#)
49. Plotka-Wasyłka, J.; Frankowski, M.; Simeonov, V.; Polkowska, Ż.; Namieśnik, J. Determination of Metals Content in Wine Samples by Inductively Coupled Plasma-Mass Spectrometry. *Molecules* **2018**, *23*, 2886. [\[CrossRef\]](#)
50. *Guideline: Potassium Intake for Adults and Children*; World Health Organization: Geneva, Switzerland, 2012.
51. Kawasaki, T.; Itoh, K.; Kawasaki, M. Reduction in Blood Pressure with a Sodium-Reduced, Potassium- and Magnesium-Enriched Mineral Salt in Subjects with Mild Essential Hypertension. *Hypertens. Res.* **1998**, *21*, 235–243. [\[CrossRef\]](#)
52. Campbell, I. Macronutrients, Minerals, Vitamins and Energy. *Anaesth. Intensive Care Med.* **2014**, *15*, 344–349. [\[CrossRef\]](#)
53. Seeman, E.; Boonen, S.; Borgström, F.; Vellas, B.; Aquino, J.-P.; Semler, J.; Benhamou, C.-L.; Kaufman, J.-M.; Reginster, J.-Y. Five Years Treatment with Strontium Ranelate Reduces Vertebral and Nonvertebral Fractures and Increases the Number and Quality of Remaining Life-Years in Women over 80 Years of Age. *Bone* **2010**, *46*, 1038–1042. [\[CrossRef\]](#)
54. Levent, H.; Sayaslan, A.; Yeşil, S. Physicochemical and Sensory Quality of Gluten-free Cakes Supplemented with Grape Seed, Pomegranate Seed, Poppy Seed, Flaxseed, and Turmeric. *J. Food Process. Preserv.* **2021**, *45*, e15148. [\[CrossRef\]](#)
55. Elkatry, H.O.; Ahmed, A.R.; El-Beltagi, H.S.; Mohamed, H.I.; Eshak, N.S. Biological Activities of Grape Seed By-Products and Their Potential Use as Natural Sources of Food Additives in the Production of Balady Bread. *Foods* **2022**, *11*, 1948. [\[CrossRef\]](#)
56. Oprea, O.B.; Popa, M.E.; Apostol, L.; Gaceu, L. Research on the Potential Use of Grape Seed Flour in the Bakery Industry. *Foods* **2022**, *11*, 1589. [\[CrossRef\]](#)
57. EFSA Panel on Dietetic Products, Nutrition and Allergies (NDA). Scientific Opinion on Dietary Reference Values for Copper: Dietary Reference Values for Copper. *EFSA J.* **2015**, *13*, 4253. [\[CrossRef\]](#)
58. Duplay, J.; Semhi, K.; Errais, E.; Imfeld, G.; Babcsanyi, I.; Perrone, T. Copper, Zinc, Lead and Cadmium Bioavailability and Retention in Vineyard Soils (Rouffach, France): The Impact of Cultural Practices. *Geoderma*, 2014; 230–231, 318–328. [\[CrossRef\]](#)
59. EFSA Panel on Contaminants in the Food Chain; Schrenk, D.; Bignami, M.; Bodin, L.; Chipman, J.K.; del Mazo, J.; Grasl-Kraupp, B.; Hogstrand, C.; Hoogenboom, L.R.; Leblanc, J.-C.; et al. Scientific Opinion on the update of the risk assessment of nickel in food and drinking water. *EFSA J.* **2022**, *18*, 6268. [\[CrossRef\]](#)
60. Commission Regulation (EC). No 1881/2006 of 19 December 2006 setting maximum levels for certain contaminants in foodstuffs. *Off. J. Eur. Union* **2006**. Available online: <https://eur-lex.europa.eu/LexUriServ/LexUriServ.do?uri=OJ:L:2006:364:0005:0024:EN:PDF> (accessed on 10 December 2022).
61. Berk, E.; Hamzalioglu, A.; Gokmen, V. Investigations on the Maillard Reaction in Sesame (*Sesamum indicum* L.) Seeds Induced by Roasting. *J. Agric. Food Chem.* **2019**, *67*, 4923–4930. [\[CrossRef\]](#)
62. Parker, J.K. Introduction to aroma compounds in foods. In *Flavour Development, Analysis and Perception in Food and Beverages*, Woodhead Publishing Series; Parker, J.K., Elmore, S., Methven, L., Eds.; Woodhead Publishing: Sawston, UK, 2015; Chapter 1, pp. 6–10.
63. Zou, Y.; Gaida, M.; Franchina, F.A.; Stefanuto, P.H.; Focant, J.F. Distinguishing between Decaffeinated and Regular Coffee by HS-SPME-GC x GC-TOFMS, Chemometrics, and Machine Learning. *Molecules* **2022**, *27*, 1806. [\[CrossRef\]](#)
64. Gernat, D.C.; Brouwer, E.; Ottens, M. Aldehydes as Wort Off-Flavours in Alcohol-Free Beers—Origin and Control. *Food Bioproc. Tech.* **2020**, *13*, 195–216. [\[CrossRef\]](#)

65. Smit, A.B.; Engels, W.J.M.; Smit, G. Branched chain aldehydes: Production and breakdown pathways and relevance for flavour in foods. *Appl. Microbiol. Biotechnol.* **2009**, *81*, 987–999. [\[CrossRef\]](#)
66. Siegmund, B.; Murkovic, M. Changes in chemical composition of pumpkin seeds during the roasting process for production of pumpkin seed oil (Part 2: Volatile compounds). *Food Chem.* **2004**, *84*, 367–374. [\[CrossRef\]](#)
67. Poisson, L.; Blank, I.; Dunkel, A.; Hofmann, T. The Chemistry of Roasting-Decoding Flavor Formation. In *The Craft and Science of Coffee*; Elsevier: Amsterdam, The Netherlands, 2017; pp. 273–309. ISBN 9780128035580.
68. Perez Locas, C.A.; Yaylayan, V. Origin and Mechanistic Pathways of Formation of the Parent Furan-A Food Toxicant. *J. Agric. Food Chem.* **2004**, *52*, 6830–6836. [\[CrossRef\]](#)
69. Bail, S.; Stuebiger, G.; Krist, S.; Unterweger, H.; Buchbauer, G. Characterisation of various grape seed oils by volatile compounds, triacylglycerol composition, total phenols and antioxidant capacity. *Food Chem.* **2008**, *108*, 1122–1132. [\[CrossRef\]](#)
70. Ridgway, K. Analysis of taints and off-flavours. In *Flavour Development, Analysis and Perception in Food and Beverages*, Woodhead Publishing Series; Parker, J.K., Elmore, S., Methven, L., Eds.; Woodhead Publishing: Sawston, UK, 2015; Chapter 4; pp. 63–79.
71. Adamiec, J.; Rossner, J.; Velisek, J.; Cejpek, K.; Savel, J. Minor Strecker degradation products of phenylalanine and phenylglycine. *Eur. Food Res. Technol.* **2001**, *212*, 135–140. [\[CrossRef\]](#)
72. Xiao, Z.; Dai, S.; Niu, Y.; Yu, H.; Zhu, J.; Tian, H.; Gu, Y. Discrimination of Chinese Vinegars Based on Headspace Solid-Phase Microextraction-Gas Chromatography Mass Spectrometry of Volatile Compounds and Multivariate Analysis. *J. Food Sci.* **2011**, *76*, 8. [\[CrossRef\]](#)
73. Zakidou, P.; Plati, F.; Matsakidou, A.; Varka, E.-M.; Blekas, G.; Paraskevopoulou, A. Single Origin Coffee Aroma: From Optimized Flavor Protocols and Coffee Customization to Instrumental Volatile Characterization and Chemometrics. *Molecules* **2021**, *26*, 4609. [\[CrossRef\]](#)
74. Yanfang, Z.; Wenyi, T. Flavor and taste compounds analysis in Chinese solid fermented soy sauce. *Afr. J. Biotechnol.* **2009**, *8*, 673–681.
75. Dorfner, R.; Ferge, T.; Kettrup, A.; Zimmermann, R.; Yeretdzian, C. Real-Time Monitoring of 4-Vinylguaiacol, Guaiacol, and Phenol during Coffee Roasting by Resonant Laser Ionization Time-of-Flight Mass Spectrometry. *J. Agric. Food Chem.* **2003**, *51*, 5768–5773. [\[CrossRef\]](#)
76. Sevindik, O.; Kelebek, H.; Rombolà, A.D.; Selli, S. Grape seed oil volatiles and odour activity values: A comparison with Turkish and Italian cultivars and extraction methods. *J. Food Sci. Technol.* **2022**, *59*, 1968–1981. [\[CrossRef\]](#)
77. Morales, M.L.; Gonzalez, A.G.; Casas, J.A.; Troncoso, A.M. Multivariate analysis of commercial and laboratory produced Sherry wine vinegars: Influence of acetification and aging. *Eur. Food Res. Technol.* **2001**, *212*, 676–682. [\[CrossRef\]](#)
78. Câmara, J.S.; Lourenço, S.; Silva, C.; Lopes, A.; Andrade, C.; Perestrelo, R. Exploring the potential of wine industry by-products as source of additives to improve the quality of aquafeed. *Microchem. J.* **2020**, *155*, 104758. [\[CrossRef\]](#)
79. Limacher, A.; Kerler, J.; Davidek, T.; Schmalzried, F.; Blank, I. Formation of Furan and Methylfuran by Maillard-Type Reactions in Model Systems and Food. *J. Agric. Food Chem.* **2008**, *56*, 3639–3647. [\[CrossRef\]](#)
80. FDA. Available online: <https://www.fda.gov> (accessed on 15 November 2022).
81. Chang, S.S.; Smouse, T.H.; Krishnamurthy, R.G.; Mookherjee, B.D.; Reddy, R.B. Isolation and identification of 2-pentyl-furan as contributing to the reversion flavour of soybean oil. *Chem. Ind.* **1966**, 1926–1927.
82. Vichi, S.; Pizzale, L.; Conte, L.S.; Buxaderas, S.; Lo'pezTamames, E. Solid-phase microextraction in the analysis of virgin olive oil volatile fraction: Modifications induced by oxidation and suitable markers of oxidative status. *J. Agric. Food Chem.* **2003**, *51*, 6564–6571.
83. IARC. *Monographs on the Evaluation of Carcinogenic Risks to Humans*; International Agency for Research on Cancer: Lyon, France, 1995; Volume 63, pp. 3194–3407.
84. Yaylayan, V.; Wnorowski, A. The role of L-serine and L-threonine in the generation of sugar-specific reactive intermediates during Maillard reaction. In *Food Flavors and Chemistry Advances of the New Millennium*; Spanier, A., Shahidi, F., Parliment, T., Mussinan, C., Ho, C.-T., Contis, E., Eds.; Royal Society of Chemistry: Cambridge, UK, 2001; pp. 313–317.
85. Patel, R.; Panya, H.N. Production of acetic acid from molasses by fermentation process. *Int. J. Adv. Res. Innov. Ideas Educ.* **2015**, *1*, 58–60.
86. Boss, P.K.; Pearce, A.D.; Zhao, Y.; Nicholson, E.L.; Dennis, E.G.; Jeffery, D.W. Potential Grape-Derived Contributions to Volatile Ester Concentrations in Wine. *Molecules* **2015**, *20*, 7845–7873. [\[CrossRef\]](#)
87. Gambetta, M.J.; Bastian, S.E.P.; Cozzolino, D.; Jeffery, D.W. Factors Influencing the Aroma Composition of Chardonnay Wines. *J. Agric. Food Chem.* **2014**, *62*, 6512–6534. [\[CrossRef\]](#)
88. Plata, C.; Millan, C.; Mauricio, J.C.; Ortega, J.M. Formation of ethyl acetate and isoamyl acetate by various species of wine yeasts. *Food Microbiol.* **2003**, *20*, 217–224. [\[CrossRef\]](#)
89. Panighel, A.; Flamini, R. Applications of Solid-Phase Microextraction and Gas Chromatography/Mass Spectrometry (SPME-GC-MS) in the Study of Grape and Wine Volatile Compounds. *Molecules* **2014**, *19*, 21291–21309. [\[CrossRef\]](#)
90. Yang, Y.; Jin, G.; Kong, C.; Liu, J.; Tao, Y. Chemical profiles and aroma contribution of terpene compounds in Meili (*Vitis vinifera* L.) grape and wine. *Food Chem.* **2019**, *283*, 155–161. [\[CrossRef\]](#)
91. Mendes-Pinto, M.M. Carotenoid breakdown products the-norispreoids- in wine aroma. *Arch. Biochem. Biophys.* **2009**, *482*, 236–245. [\[CrossRef\]](#)

92. Baumes, R.; Wirth, J.; Bureau, S.; Gunata, Y.; Razungles, A. Biogenesis of C13-norisoprenoid compounds: Experiments supportive for an apo-carotenoid pathway in grapevines. *Anal. Chim. Acta* **2002**, *458*, 3–14. [\[CrossRef\]](#)
93. Antonic, B.; Dordevic, D.; Jancikova, S.; Holeckova, D.; Tremlova, B.; Kulawik, P. Effect of Grape Seed Flour on the Antioxidant Profile, Textural and Sensory Properties of Waffles. *Processes* **2021**, *9*, 131. [\[CrossRef\]](#)
94. Rosales Soto, M.U.; Brown, K.; Ross, C.F. Antioxidant Activity and Consumer Acceptance of Grape Seed Flour-Containing Food Products: Antioxidant Activity and Consumer Acceptance of Grape Seed Flour. *Int. J. Food Sci. Technol.* **2012**, *47*, 592–602. [\[CrossRef\]](#)
95. Hoyer, C., Jr.; Ross, C.F. Total Phenolic Content, Consumer Acceptance, and Instrumental Analysis of Bread Made with Grape Seed Flour. *J. Food Sci.* **2011**, *76*, S428–S436. [\[CrossRef\]](#)
96. Spanghero, M.; Salem, A.Z.M.; Robinson, P.H. Chemical Composition, Including Secondary Metabolites, and Rumen Fermentability of Seeds and Pulp of Californian (USA) and Italian Grape Pomaces. *Anim. Feed Sci. Technol.* **2009**, *152*, 243–255. [\[CrossRef\]](#)
97. Johnson, C.M. Differential Scanning Calorimetry as a Tool for Protein Folding and Stability. *Arch. Biochem. Biophys.* **2013**, *531*, 100–109. [\[CrossRef\]](#)
98. Ojeda-Galván, H.J.; Hernández-Arteaga, A.C.; Rodríguez-Aranda, M.C.; Toro-Vazquez, J.F.; Cruz-González, N.; Ortiz-Chávez, S.; Comas-García, M.; Rodríguez, A.G.; Navarro-Contreras, H.R. Application of Raman Spectroscopy for the Determination of Proteins Denaturation and Amino Acids Decomposition Temperature. *Spectrochim. Acta A Mol. Biomol. Spectrosc.* **2023**, *285*, 121941. [\[CrossRef\]](#)
99. Şen, D.; Gökmen, V. Kinetic Modeling of Maillard and Caramelization Reactions in Sucrose-Rich and Low Moisture Foods Applied for Roasted Nuts and Seeds. *Food Chem.* **2022**, *395*, 133583. [\[CrossRef\]](#)
100. Weiss, I.M.; Muth, C.; Drumm, R.; Kirchner, H.O.K. Thermal decomposition of the amino acids glycine, cysteine, aspartic acid, asparagine, glutamic acid, glutamine, arginine and histidine. *BMC Biophys.* **2018**, *11*, 2. [\[CrossRef\]](#)
101. Salema, A.A.; Ting, R.M.W.; Shang, Y.K. Pyrolysis of blend (oil palm biomass and sawdust) biomass using TG-MS. *Bioresour. Technol.* **2019**, *274*, 439–446. [\[CrossRef\]](#)
102. Wang, S.; Dai, G.; Yang, H.; Luo, Z. Lignocellulosic Biomass Pyrolysis Mechanism: A State-of-the-Art Review. *Prog. Energy Combust. Sci.* **2017**, *62*, 33–86. [\[CrossRef\]](#)
103. Ding, Y.; Huang, B.; Li, K.; Du, W.; Lu, K.; Zhang, Y. Thermal Interaction Analysis of Isolated Hemicellulose and Cellulose by Kinetic Parameters during Biomass Pyrolysis. *Energy* **2020**, *195*, 117010. [\[CrossRef\]](#)
104. Yang, H.; Yan, R.; Chin, T.; Liang, D.T.; Chen, H.; Zheng, C. Thermogravimetric Analysis–Fourier Transform Infrared Analysis of Palm Oil Waste Pyrolysis. *Energy Fuels* **2004**, *18*, 1814–1821. [\[CrossRef\]](#)
105. Zhao, C.; Jiang, E.; Chen, A. Volatile Production from Pyrolysis of Cellulose, Hemicellulose and Lignin. *J. Energy Inst.* **2017**, *90*, 902–913. [\[CrossRef\]](#)
106. Yeo, J.Y.; Chin, B.L.F.; Tan, J.K.; Loh, Y.S. Comparative Studies on the Pyrolysis of Cellulose, Hemicellulose, and Lignin Based on Combined Kinetics. *J. Energy Inst.* **2019**, *92*, 27–37. [\[CrossRef\]](#)
107. Oreopoulou, V.; Tzia, C. Utilization of Plant By-Products for the Recovery of Proteins, Dietary Fibers, Antioxidants, and Colorants. In *Utilization of By-Products and Treatment of Waste in the Food Industry*; Springer: New York, NY, USA, 2006; pp. 209–232.
108. Villanueva-Suárez, M.J.; Redondo-Cuenca, A.; Rodríguez-Sevilla, M.D.; de las Heras Martínez, M. Characterization of Nonstarch Polysaccharides Content from Different Edible Organs of Some Vegetables, Determined by GC and HPLC: Comparative Study. *J. Agric. Food Chem.* **2003**, *51*, 5950–5955. [\[CrossRef\]](#)
109. Figuerola, F.; Hurtado, M.L.; Estévez, A.M.; Chiffelle, I.; Asenjo, F. Fibre Concentrates from Apple Pomace and Citrus Peel as Potential Fibre Sources for Food Enrichment. *Food Chem.* **2005**, *91*, 395–401. [\[CrossRef\]](#)
110. Dhingra, D.; Michael, M.; Rajput, H.; Patil, R.T. Dietary Fibre in Foods: A Review. *J. Food Sci. Technol.* **2012**, *49*, 255–266. [\[CrossRef\]](#)
111. Thebaudin, J.Y.; Lefebvre, A.C.; Harrington, M.; Bourgeois, C.M. Dietary fibres: Nutritional and technological interest. *Trends Food Sci. Technol.* **1997**, *8*, 41–48. [\[CrossRef\]](#)
112. Subiria-Cueto, R.; Coria-Oliveros, A.J.; Wall-Medrano, A.; Rodrigo-García, J.; González-Aguilar, G.A.; Martínez-Ruiz, N.d.R.; Alvarez-Parrilla, E. Antioxidant Dietary Fiber-Based Bakery Products: A New Alternative for Using Plant-by-Products. *Food Sci. Technol.* **2021**, *42*, 1–16. [\[CrossRef\]](#)
113. Besbes, S.; Attia, H.; Deroanne, C.; Makni, S.; Blecker, C. Partial Replacement of Meat by Pea Fiber and Wheat Fiber: Effect on the Chemical Composition, Cooking Characteristics and Sensory Properties of Beef Burgers. *J. Food Qual.* **2008**, *31*, 480–489. [\[CrossRef\]](#)

**Disclaimer/Publisher’s Note:** The statements, opinions and data contained in all publications are solely those of the individual author(s) and contributor(s) and not of MDPI and/or the editor(s). MDPI and/or the editor(s) disclaim responsibility for any injury to people or property resulting from any ideas, methods, instructions or products referred to in the content.